ACS OMEGA

Open Access

This article is licensed under CC-BY-NC-ND 4.0

http://pubs.acs.org/journal/acsodf

Article

Catalytic Conversion of Nonequilibrium Hydrogen and Nitrogen Species from Low-Pressure Inductively Coupled Plasma to Ammonia

Rok Zaplotnik,* Alenka Vesel, Parameswaram Ganji, Gregor Primc, Miha Čekada, Gregor Dolanc, and Miran Mozetič

Cite This: https://doi.org/10.1021/acsomega.6c01120

Read Online

ACCESS | Metrics & More | Article Recommendations | Supporting Information

ABSTRACT: Gas conversion between hydrogen (H_2), nitrogen (N_2), and ammonia (NH_3) is a scientific topic of interest in both methods for low-temperature synthesis of ammonia and energy-efficient production of hydrogen for powering fuel cells. The efficiency of catalysts for ammonia synthesis at room temperature was evaluated. A mixture of hydrogen and nitrogen with a ratio in a broad range between 1.5:1 and 80:1 was passed through a plasma sustained by inductively coupled radio frequency discharge in the H mode at a power of 700 W and pressures between 40 and 100 Pa. Several catalysts were placed in the flowing afterglow where the H and N densities were of the order of 10^{21} m^{-3}, and the conversion efficiency (η) was evaluated. The efficiency increased almost linearly with increasing enthalpy of nitride formation. The best results were observed for copper, for which the conversion was almost twice the value in the same system without the catalyst. The efficiency of NH_3 production by the conversion of N atoms into NH_3 molecules versus the gas mixture exhibited a broad maximum and was as large as $\eta \approx 29\%$ in the mixture of hydrogen and nitrogen between 3:1 and 10:1.

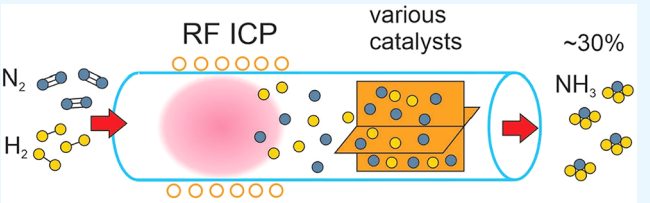

Downloaded via INST JOZEF STEFAN on May 14, 2026 at 10:20:21 (UTC).
See https://pubs.acs.org/sharingguidelines for options on how to legitimately share published articles.

INTRODUCTION

Conversion of hydrogen and nitrogen to ammonia has been a subject of scientific interest for over a century. The standard Haber-Bosch process has been optimized and is nowadays used for ammonia synthesis on an industrial scale.[1−3] The technology runs at high temperatures and pressures, which enables appropriate dissociative adsorption of nitrogen molecules on the catalyst surface, coadsorption of hydrogen, and synthesis of ammonia.[4,5] The technology could be used in reactors of various sizes and geometries, but only large-scale reactors are used for the mass production of ammonia.[4,5] Decades ago, it was proposed to synthesize ammonia at much lower pressures and temperatures.[6−9] One of the possible solutions for synthesizing ammonia at room temperature is the application of plasma catalysis.[10]

Nonequilibrium gaseous plasma is a suitable medium for gas conversion because the gas does not have to be heated to a high temperature. Instead, the potential barrier for the dissociative adsorption of nitrogen on a catalyst surface is lowered by impinging molecules of moderate potential energy. Such molecules are nitrogen metastables, for example, in the ($A\ ^3\sum_u^+$) state of potential energy as large as 6.2 eV.[11] Alternatively, highly excited vibrational states of nitrogen have been proposed, as the vibrational temperature of nitrogen molecules is several 1000 K even in weakly ionized plasma sustained at a low power density.[11,12] Yet another option is dissociation of nitrogen molecules in the gaseous plasma,[13,14] so that the N atoms impinging on the catalyst surface remain weakly bonded on a catalyst surface for a period long enough to interact with hydrogen atoms or molecules, say several ns (nanoseconds). Hydrogen molecules are also dissociated in nonequilibrium plasma,[15,16] and the concentration of H atoms is much larger than the N atoms at comparable discharge parameters because of the large difference in the dissociation energies. The dissociation energies are 9.8 and 4.5 eV for nitrogen and hydrogen molecules in the ground state, respectively. Taking into account the electron energy distribution function in nonequilibrium plasma, which is close to Maxwellian with an exponential high-energy tail, the production of H atoms in plasma should be much larger than the production of N atoms at the same discharge conditions. Nonequilibrium plasma thus seems attractive for the conversion of hydrogen and nitrogen to ammonia, but there are both theoretical and practical limitations.

Regardless of the gas temperature, nonequilibrium plasma could be sustained in a very broad range of pressures, from less than 1 Pa to over 1 bar. Low-pressure plasmas are homogeneous in a large volume, whereas atmospheric pressure plasmas are often in the form of localized streamers.[17]

Received: January 29, 2026
Revised: March 10, 2026
Accepted: April 8, 2026

© XXXX The Authors. Published by American Chemical Society

Atmospheric pressure plasmas could also be at least quasi-uniform in a large volume, but not at low temperatures. The reason is the abundance of gas-phase collisions, whose frequency increases with increasing pressure.[17] Of particular importance are three-body collisions, whose frequency increases with the square of the pressure.[18] It is over MHz at atmospheric pressure and as low as mHz (0.001 three-body collision per second) at 1 Pa. While inelastic collisions between free electrons of elevated energy and gaseous molecules lead to the formation of useful plasma species (atoms, electronically and vibrationally excited molecules), the superelastic collisions between plasma species in the gas phase lead to the loss of desired plasma species. Furthermore, the energy released at a superelastic collision heats the gas. Opposite, at least some gas-phase collisions will result in the formation of ammonia molecules. This channel for the production of ammonia is, however, less efficient than the gas-phase recombination of atoms to form parent molecules, so atmospheric pressure reactors for plasma synthesis of ammonia are usually equipped with catalysts.[19] The main exothermic reactions in the gas phase of plasma sustained at atmospheric pressure (and around it) can be written as follows:

$$N + N + N_2 \rightarrow N_2 + N_2 \text{or} N + N + H_2 \rightarrow N_2 + H_2 \quad (1)$$

$$H + H + H_2 \rightarrow H_2 + H_2 \text{or} H + H + N_2 \rightarrow H_2 + N_2 \quad (2)$$

$$N + H + N_2 \rightarrow NH + N_2 \text{or} NH + H + N_2 \rightarrow NH_2 + N_2 \text{or} NH_2 + H + N_2 \rightarrow NH_3 + N_2 \quad (3)$$

$$NH + H_2 + N_2 \rightarrow NH_3 + N_2 \text{or} NH + H_2 + H_2 \rightarrow NH_3 + H_2 \quad (4)$$

The molecules involved in the gas-phase collisions stated above may also be excited. Other reactions apart from (1−4) are likely to occur in the gas phase at elevated pressures, such as atmospheric pressure.[20,21] The exothermic gas-phase reactions should involve a third body to satisfy the requirement for conservation of energy and momentum. Charged particles are also lost in the gas phase at atmospheric pressure by three-body collisions.

The loss of radicals and gas heating by three-body collisions in the gas phase is marginal at low-pressure conditions. As already mentioned, their frequency is marginal if the pressure is below 1 mbar. The predominant loss of plasma species at low pressure is due to the surface reactions.[22] The charged particles impinging on a surface facing the plasma will neutralize at a very high probability. The free atoms will adsorb on surfaces and will react with impinging atoms. The surface reaction will cause either the formation of parent molecules because of the heterogeneous surface recombination or ammonia.[20] The most important surface reactions are therefore

$$N_s + N_{imp} \rightarrow N_2 \text{or} N_s + N_s \rightarrow N_2 \quad (5)$$

$$H_s + H_{imp} \rightarrow H_2 \text{or} H_s + H_s \rightarrow H_2 \quad (6)$$

$$N_s + 3H_{imp} \rightarrow NH_3 \text{or} N_s + H_s + H_2 \rightarrow NH_3 \text{etc} \quad (7)$$

The subscript "s" in the above reactions denotes an atom adsorbed on the surface, and "imp" an atom impinging on the surface. Other surface reactions are likely to occur, too. There is no need for a third particle in reactions 5−8 because the surface atoms of the solid material do the job (ensuring energy and momentum conservation). The reactions 5−8 are exothermic and will heat the material facing the plasma. The gas will not be heated directly, but only by accommodation of gaseous molecules on the materials, which are heated due to exothermic surface reactions. The energy efficiency of plasma technologies, as well as the ability to sustain plasma in large volumes, are the main reasons for the predominant industrial application of low-pressure plasmas.[23]

Both atmospheric and low-pressure synthesis of ammonia have a theoretical drawback, which arises from the fact that the dissociation energy of ammonia is much smaller than that of nitrogen. The production of ammonia may be adequate, but the NH_3 molecules are likely to be dissociated in plasma, and probably converted back to N_2 and H_2 before escaping the glowing plasma, where free electrons of large enough energy for ammonia dissociation abound.

Another drawback is the high vapor pressure of ammonia. It is about 10 bar at room temperature, and 4 bar at 0 °C. The critical point of ammonia is at 132 °C and 113 bar. Ammonia synthesized at higher temperatures (like in the Haber-Bosch process) should be cooled well to facilitate liquification, which is essential for the separation of the liquid ammonia from gaseous nitrogen and hydrogen. Heating (for synthesis) and cooling (for separation) are energy-demanding, so the Haber-Bosch process consumes a lot of energy.

Low-pressure plasmas operate well below the ammonia saturation vapor pressure, so this technique is not feasible for the separation of ammonia from remaining nitrogen and hydrogen. Obviously, the gas mixture should be pressurized after the synthesis of ammonia by low-pressure plasma. Pressurization by adiabatic compression will heat the gas mixture, and the pressurized gas will have to be cooled to enable separation, so the synthesis by low-pressure plasma technology will also be energy-demanding. The synthesis of ammonia by using low-pressure nonequilibrium plasma is thus not very attractive for mass application, but useful for studying the basic process on the surface conversion of nitrogen and hydrogen species with high potential energy (like N and H atoms, N_2 metastables, and vibrationally excited N_2 molecules). As explained above, the low-pressure reactions occur practically only on the surfaces of materials (and not in the gas phase).

EXPERIMENTAL DETAILS

Plasma Reactor

This work aims to study the conversion of nitrogen and hydrogen to ammonia on selected materials under low pressure and at room temperature. We used the experimental system illustrated in Figure 1. The discharge tube is made from borosilicate glass. It is 75 cm long and has an inner diameter of 36 mm. The discharge tube is fixed hermetically tight on standard KF40 flanges. It is pumped through a series of vacuum elements (not shown in Figure 1) with a two-stage rotary pump with a nominal pumping speed of 80 m^3/h. The conductivity of vacuum elements between the discharge tube and the vacuum pump at a pressure of 1 mbar is estimated to be about 50 m^3/h, so the effective pumping speed at the end of the discharge tube toward the pump duct is approximately 31 m^3/h. Taking into account a negligible pressure gradient along the discharge tube, the gas speed through the discharge tube is estimated to

$$v_{drift} = S_{eff}/A = 8 m/s \quad (8)$$

https://doi.org/10.1021/acsomega.6c01120
ACS Omega XXXX, XXX, XXX−XXX

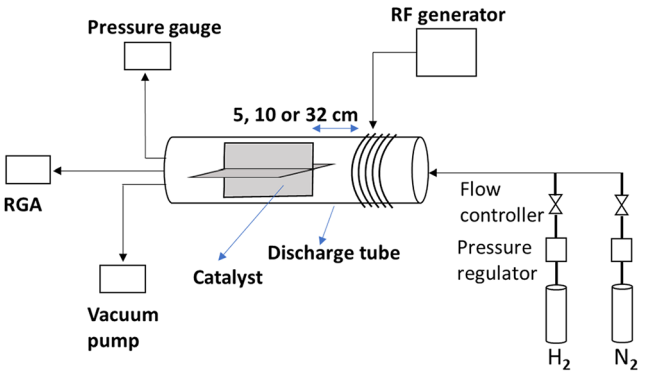

Figure 1. Schematic of the experimental setup.

Here, v_{drift} is the gas speed through the discharge tube ("drift velocity"), S_{eff} is the effective pumping speed (31 m^3/h), and A is the cross-section of the discharge tube (approximately 10 cm^2).

Gases are introduced into the discharge tube on the opposite side through flow controllers and a few vacuum elements (not shown in Figure 1). We used Aera FC-7700 Mass Flow Controllers. The gas purity was 99.999 and 99.9995% for nitrogen and hydrogen, respectively. The pressure at the end of the discharge tube (toward the pump duct) was measured with the MKS Baratron 722A absolute pressure gauge.

Plasma was sustained in the discharge tube using an inductively coupled radio frequency RF generator (Cesar 1310, Advanced Energy). The generator was connected to a 6-turn excitation coil through a matching network (ICP Variomatch, Advanced Energy). Plasma was in the E mode at low discharge powers, but transformed to H mode at a power of approximately 700 W. Details about the plasma behavior in both modes are explained elsewhere.[24] Briefly, the discharge coupling is predominantly capacitive in the E mode and inductive in the H mode. The plasma luminosity is much larger in the H mode because of the efficient coupling between the RF field and the plasma electrons. The H-mode plasma does not spread along the entire discharge tube, but is limited to the volume within the RF coil. The length of plasma in the H mode was approximately 8 cm. Taking into account the drift velocity from eq 8, the gas residence time in the dense plasma in the H mode was

$$t = l/v_{drift} = 10\text{ms} \quad (9)$$

Here, l is the length of the plasma in the H mode, and v_{drift} is the drift velocity calculated according to eq 8. There is barely visible diffusing plasma which propagates a few cm from the coil toward the pump duct, but there is no stray capacitance between the coil and the flange at the edge of the discharge tube. The gas in the discharge tube between the coil and the pump duct is thus nonequilibrium, but almost free from electrons, which might otherwise cause dissociation of synthesized ammonia molecules. Such a state of the gas is often called "flowing afterglow" and is rich in relatively stable plasma species (such as atoms) but free from energetic electrons.

Plasma Characterization and Measurement of NH_3 Production

The gas composition at the end of the discharge tube was analyzed using a differentially pumped Residual Gas Analyzer (RGA), Pfeiffer Vacuum PrismaPlus QMG 220. The RGA was connected to the discharge tube through a narrowed glass tube (inner diameter 0.8 mm), which provided the pressure reduction necessary to maintain the pressure in the RGA chamber below 10^{-5} mbar. Each RGA measurement was performed long enough to allow the ammonia-related peaks in the mass spectra to stabilize. All RGA spectra were acquired in the range of 0−35 Da. The residual atmosphere in the ionization chamber of the RGA consisted predominantly of water vapor. Water vapor partially dissociates in the ionization chamber. The OH^+ ions overlap in the mass spectrum with NH_3^+, so their contribution at m = 17 Da was deduced from the spectra used to calculate the ammonia concentration. Ammonia exhibits a strong peak also at m/z 16 Da, so it is feasible to distinguish between the RGA signal arising from the residual atmosphere and ammonia in the ionization chamber. Details on the method for calibration of RGA for proper determination of the ammonia concentration are presented elsewhere.[25] The RGA calibration curve for ammonia is presented in Supporting Information in Figure S1.

The density of N and H atoms in the afterglow was measured with calibrated catalytic probes. We used homemade probes which are capable of measuring the atom densities in pure gases, but not in the mixture of hydrogen and nitrogen. More details about the probes can be found elsewhere.[26] Briefly, a catalytic probe measures the heat dissipated on a selected catalyst due to the heterogeneous surface recombination according to (5) and (6). The temporal and spatial resolution of the catalytic probes is approximately 5 s and 3 mm, respectively, and the accuracy is approximately 30%.

Preparation of Catalysts

Different materials (Fe, Pd, Ru, Ni, Zn, Pt, Cu, Ti) that are supposed to be catalysts for ammonia synthesis according to reaction 7 were mounted into the afterglow part of the discharge tube as shown in Figure 1. Thin films of the above-mentioned materials were deposited on the rectangular stainless-steel substrates by sputter deposition using high-purity targets. The stainless steel substrates were coated from both sides, so their surface was fully covered by the deposit with a thickness of approximately 100 nm. The morphology of the coated catalysts was examined using scanning electron microscopy (SEM), and no significant differences were observed between the samples. The SEM images for all catalysts are presented in Figure S2 in the Supporting Information. The rectangular stainless-steel substrates were assembled to form a cross (as illustrated in Figure 1) with a total surface area of 168 cm^2 (dimensions of the individual rectangular

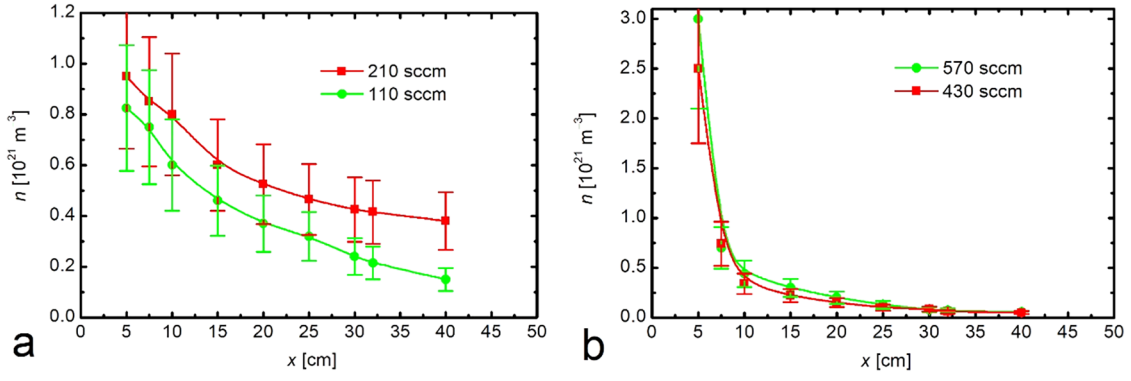

Figure 2. Density of nitrogen (a) and hydrogen (b) atoms along the discharge tube versus the distance from the end of the RF coil. The parameter is the gas flow.

https://doi.org/10.1021/acsomega.6c01120
ACS Omega XXXX, XXX, XXX−XXX

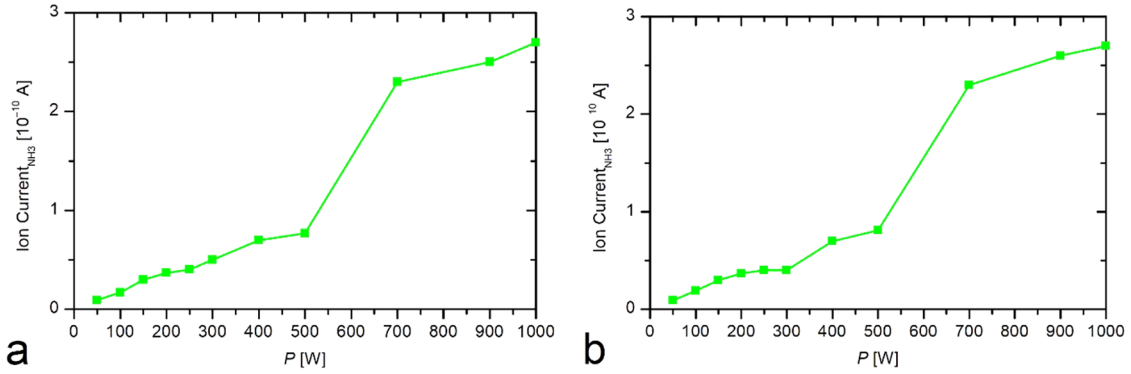

Figure 3. Intensity of the RGA ammonia peak versus RF power at: (a) 110 sccm of nitrogen and 360 sccm of hydrogen, and (b) at 70 sccm of nitrogen and 430 sccm of hydrogen.

stainless-steel substrates were 12 cm in length and 3.5 cm in width and height). The distance between the end of the excitation coil and the beginning of the stainless-steel cross covered with a catalyst was either 5, 10, or 32 cm (Figure 1).

The catalysts' surfaces were analyzed with X-ray photoelectron spectroscopy (XPS) to prove the presence of the catalyst. XPS instrument model PHI Genesis, from ULVAC-PHI (Physical Electronics Ltd., Munich, Germany) was used. Survey spectra were measured and analyzed by Multipak software (version 9.9.2) from Ulvac (Kanagawa, Japan) to determine the elemental composition. The measured surface composition of the catalysts before and after ammonia synthesis is presented in the Supporting Information (Tables S1 and S2).

RESULTS AND DISCUSSION

NH_3 Production in a Plasma Reactor Without the Catalyst

Densities of N and H Atoms in Plasma. The density of N and H atoms in the plasma afterglow (at the position of the catalyst in Figure 1) was measured versus the distance from the RF coil at 700 W and two gas flows. The results are shown in Figure 2. Figure 2a shows the distribution of atomic nitrogen along the afterglow segment of the discharge tube. The N atom density decreases with increasing distance from the glowing plasma in the H mode, which is explained by heterogeneous recombination of N atoms to parent molecules on the glass surface. Borosilicate glass is not renowned for facilitating surface recombination of N atoms, so the curves in Figure 2a are not particularly steep. Furthermore, the gas speed is rather large as disclosed in eq 8. The decay of the N atom density is somewhat larger at a lower flow (green curve in Figure 2a), where the N atom density drops by a factor of 5.5 from position x = 5 cm to 40 cm. For the higher nitrogen flow of 210 sccm (standard cubic centimeters per minute), the factor is 2.5. The difference is explained by lower pressure at lower flow rates, which facilitates diffusion and, thus, surface recombination on borosilicate glass.

The density of H atoms along the glass tube is shown in Figure 2b. The initial density (at x = 5 cm) is larger than the density of N atoms, but the curves in Figure 2b are much steeper than for the case of N atoms (Figure 2a). The reason is a larger coefficient for heterogeneous surface recombination of H atoms on the borosilicate glass.[27] At the chosen conditions, the H atom density becomes equal to the N atom density at a distance of x = 7 cm. The H atom density becomes marginal at large distances from its source, i.e., plasma in the H mode.

Comparison between Figure 2a and b indicates that the surface recombination of H atoms on the borosilicate tube may limit the production of ammonia on the catalyst. However, the borosilicate surface may alter the efficiency of H atom surface recombination when a mixture of hydrogen and nitrogen is introduced into the discharge tube, so the curve shown in Figure 2b should be interpreted with caution. We used a broad range of gas mixtures to probe ammonia production, even though the loss of H atoms along the path from the glowing plasma to the catalyst was substantial.

Effect of an RF Power on NH_3 Production. To identify the optimal RF power, we conducted experiments on ammonia production in the discharge tube without a catalyst as a function of RF power. The forward RF power was varied between 50 and 1000 W. The RGA signal is shown in Figure 3 for two different gas mixtures. As expected, ammonia production increases with increasing discharge power. The increase is fairly linear up to a discharge power of 500 W. Plasma is in the E mode in this power range. Increasing the discharge power beyond 500 W causes plasma instabilities typical for the transition between two distinguished modes in inductively coupled discharges.[24] The plasma became stable again at the discharge power of 700 W, where the discharge was in the H mode. The transition from the E and H modes causes an increase in the ammonia production by a factor of approximately 5, regardless of the gas mixture. Further increase in the discharge power (beyond 700 W) caused a gradual increase in the ammonia production, but the slope is modest. Based on the results shown in Figure 3, we selected the discharge power of 700 W for systematic measurements.

Effect of the Gas Flow of H_2 and N_2 on NH_3 Production. Figure 3 indicates that the concentration of gases in the H_2 and N_2 mixture does not influence the production of ammonia much. However, we performed systematic measurements to evaluate the ammonia synthesis in various gas mixtures at various flows. The synthesis of ammonia versus the concentration of gases in the H_2 and N_2 mixture was measured in the discharge tube in the absence of the catalyst. Figure 4 shows the ammonia RGA signal at m/z = 17 Da versus the ratio between the hydrogen and nitrogen flows. The hydrogen flow was fixed at 570 sccm, and the nitrogen flow was varied between 7 and 210 sccm. There is a broad maximum that peaks at the gas mixture of approximately H_2:N_2 = 4:1. Therefore, the curves in Figure 4 indicate that the hydrogen concentration in the gas mixture does not dictate the ammonia synthesis as long as it is in a reasonable range. Furthermore, hydrogen flow has only a marginal effect on ammonia production. We chose the H_2 flow of 570 sccm for experiments with catalysts.

https://doi.org/10.1021/acsomega.6c01120
ACS Omega XXXX, XXX, XXX−XXX

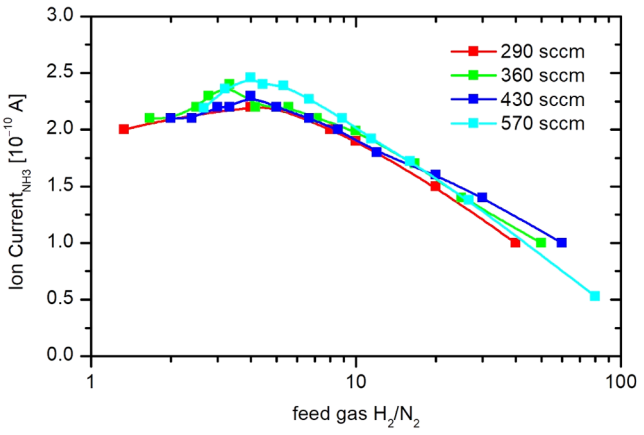

Figure 4. Intensity of the RGA ammonia peak versus the ratio between hydrogen and nitrogen feed gas at 700 W. Hydrogen flow is the parameter.

NH_3 Production in a Plasma Reactor Loaded With Various Catalysts

Systematic measurements of the ammonia production were performed in the discharge chamber loaded with various sputtered metal catalysts (Fe, Ni, Cu, Pt, Pd, Ti, Zn or Ru) at the position indicated in Figure 1. The distance between the RF coil and the catalyst (marked as "5, 10, 32 cm" in Figure 1) was varied. Figure 5 shows the relative ammonia production

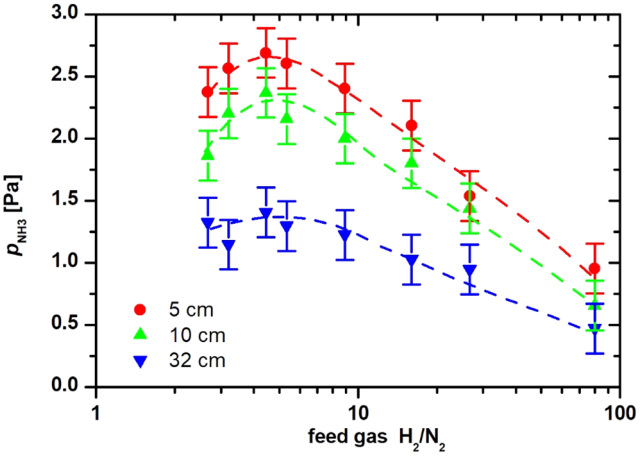

Figure 5. Partial pressure of synthesized ammonia using a zinc catalyst versus the ratio between hydrogen and nitrogen feed gas at 700 W. The distance between the coil and the catalyst is the parameter.

versus the position of the zinc catalyst in the discharge tube. Similar curves were also measured for other catalysts (Cu, Pt, Ni, Ru, Pd, Fe and Ti). The efficiency decreases with increasing distance from the source of atoms. The efficiency at the largest distance is not much different from that in the tube without the catalyst. The reason is probably a rapid decrease in the H atom density with increasing distance from the source, as shown in Figure 2b. Obviously, some ammonia is produced on the glass surfaces before the atoms reach the catalyzers. Still, the catalyst's influence on ammonia production is considerable and measurable, as shown in Figure 5.

The production of ammonia was measured for various materials that exhibit various enthalpies of formation of nitrides from −357 to +67 kJ/mol, corresponding to the binding energy from −3.7 to 0.7 eV per metal atom.[28] The catalysts were positioned at 5 cm as shown in Figure 1. Before inserting each catalyst into the experimental system, ammonia production was measured in an empty reactor under the same power and flow conditions as those used for the measurements presented in Figure 5. The same measurements were then repeated after the catalyst was introduced into the system. The results are presented in Figure S3 in the Supporting Information. Measurements in the empty reactor were consistent within the margin of error, whereas measurements obtained with different catalysts showed clear differences. To compare the contribution of each catalyst to ammonia production, the relative ammonia production (defined as the maximum partial ammonia pressure measured with the catalyst divided by the partial ammonia pressure measured in the empty reactor under the same conditions) is plotted in Figure 6 as a function of the nitrogen adsorption energy reported in

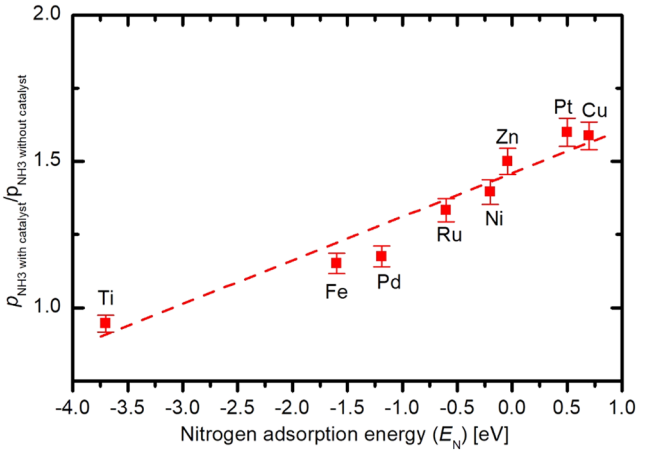

Figure 6. Relative amount of ammonia synthesized in the discharge tube using various catalysts at a position of 5 cm versus nitrogen N* adsorption energy.

the literature.[29−31] The curve is rather linear and clearly shows that the production of ammonia is favored by metals that do not form stable nitrides.[32] The nitrogen and hydrogen flows used to plot Figure 6 were 120 and 570 sccm, respectively. Interestingly, the value for titanium is even lower than for the empty chamber, indicating that the material, which forms a very stable nitride, does not enable catalytic conversion of N atoms to ammonia.[32]

Determination of the Conversion Efficiency

As already mentioned, one channel for surface synthesis of ammonia from species likely to be formed in nonequilibrium plasma sustained in a mixture of nitrogen and hydrogen is a rather weak adsorption of N atoms on the catalyst surface, and interaction of the adsorbed atom with impinging hydrogen atoms and molecules. Knowing the density of nitrogen atoms at the catalyst position (Figure 2), it is possible to estimate the efficiency of converting N atoms into ammonia molecules rather than heterogeneous surface recombination. The efficiency can be estimated by accounting for the partial pressures of ammonia and atomic nitrogen, as explained in detail elsewhere.[25] Briefly, the RGA (if calibrated well) shows the partial pressure of ammonia at the end of the glass tube in the direction toward the pump (Figure 1), and the N atom

https://doi.org/10.1021/acsomega.6c01120
ACS Omega XXXX, XXX, XXX−XXX

density is measured with the catalytic probe. The partial pressure of N atoms is calculated as

$$p_N = n_N k_B T \quad (10)$$

Here, n_N is the density of N atoms, and T is the gas temperature. If we take into account the N atom density at the position 5 cm for the flow of 210 sccm ($n_N = 0.9 \times 10^{21}$ m^{-3}), and room temperature (300 K), the partial pressure of N atoms is $p_N = 4$ Pa. The efficiency (η) of ammonia production is calculated as

$$\eta = p_{NH_3}/p_N \quad (11)$$

It should be noted that conversion efficiency (η) does not represent the exact conversion of N_2 to NH_3 as it is based on the flux of N atoms reaching the surface and assumes that these atoms are equally available for NH_3 formation. Therefore, our definition of the conversion efficiency provides an estimate of the fraction of plasma-generated N atoms detected as NH_3 in the gas phase. Consequently, this parameter should be interpreted as a relative efficiency under the given plasma conditions rather than a rigorous catalytic conversion efficiency based on a full mass balance of N_2 and H_2.

The partial pressure of ammonia (p_{NH_3}) was measured when different catalysts were immersed in the glass tube, and the efficiencies were calculated. The result is presented in Table 1.

Table 1. Efficiency η of Ammonia Production as Calculated from eq 11 for Various Surfaces

catalyst	efficiency η [%]
Ti	<1
Fe	7
Pd	8
Ru	16
Ni	19
Zn	24
Pt	29
Cu	28

The efficiency η is relatively high for copper and platinum, with a value of $\eta = 0.29$, i.e., 29%. The efficiency for other catalysts is smaller. Nitrogen atoms are thus converted to ammonia rather efficiently by surface reactions. According to literature reports on ammonia production compared with the current copper-sputtered catalyst, our present catalysts have shown a very good conversion percentage, as presented in Supporting Information (Table S3).

Here, it is worth noting that the experimental setup enabled comparisons between different catalysts and was not optimized for the synthesis of large quantities of ammonia. The results summarized in Figures 2, 5, 6, and Table 1 should serve as a guideline for further experiments. As already mentioned, the production of hydrogen and nitrogen atoms in the gas phase competes with the destruction of ammonia molecules, which have been synthesized by surface catalysis. Figure 2 clearly shows that the atom density decreases with increasing distance from the atom source; therefore, optimization of ammonia production is expected if the catalysts are placed closer to the dense plasma in the H mode. When placing the catalyst closer to the plasma, special care should be taken because the catalyst heats up more when it is closer to the plasma, and therefore, the thermal dissociation of ammonia on the surface can increase. The temperatures of the catalysts at different positions are presented in Table S4 in the Supporting Information. However, this effect is not very significant at the pressures used in our study; it becomes more prominent at higher pressures.[33] Another solution is to increase the gas speed, thereby minimizing the time the gas spends between the plasma and the catalyst. Here, it should be stressed that the theoretically maximal gas speed is the sound velocity, which is several 100 m/s, so much larger than in our experiments.

Finally, it is important to stress that the behavior shown in Figure 6 differs significantly from the "volcano curve", which is often used to evaluate conversion efficiency versus enthalpy of formation.[30,34,35] The volcano curve illustrates the conversion that occurs at equilibrium conditions, where the dissociative adsorption of nitrogen molecules in the ground electronic state is essential. When plasma catalysis is used, the molecules are already dissociated in the gas phase, so the differences between the results in Figure 6 and the volcano curve are expected. In fact, Iwamoto et al.[31] reported similar results, but the conversion rate for copper was 4 times larger than for titanium. The experimental setup in used by Iwamoto et al.[31] was completely different from our case, so the discrepancy is expected.

For comparison with previously published studies, including those summarized in our earlier review work,[10] we calculated the highest energy yield achieved in the present study. The maximum partial pressure of produced ammonia was 2.9 Pa, obtained at an effective pumping speed of approximately 50 m^3/h and an RF power of 700 W. These conditions correspond to an energy yield of approximately 1.4 gNH_3/kWh. This value exceeds the majority of the results reported in the above-mentioned review article.

CONCLUSIONS

The efficiency of conversion of N atoms into ammonia molecules was studied for various catalysts. The key result is a rather linear increase versus the enthalpy of formation of metal nitrides. The materials with highly positive enthalpy (i.e., those that do not form stable nitrides) are the best catalysts. Interestingly, the catalytic performance of copper is almost the same as that of platinum, but the cost of copper is lower, thus making it an attractive choice. The measurements of the partial pressures of ammonia and N atoms in the reactor enabled the estimation of the conversion efficiency η, which was found to be as large as 29%, meaning that 29% of N atoms impinging on the surfaces were converted to ammonia, and the rest were converted to nitrogen molecules. The results provide directions for further optimization of the catalytic surface conversion of N atoms into ammonia molecules by carefully designing the experimental setup. The results were obtained at low-pressure conditions where the loss of atoms in the gas phase is marginal, so the measured values for surface reactions are reliable. The coefficients for surface catalysis reported in this paper are mostly valid for low-pressure plasma-assisted ammonia synthesis, but may also be valid at higher pressures.

ASSOCIATED CONTENT

Supporting Information

The Supporting Information is available free of charge at https://pubs.acs.org/doi/10.1021/acsomega.6c01120.

RGA calibration curve with a description of the calibration process (Figure S1); SEM images of catalysts'

https://doi.org/10.1021/acsomega.6c01120
ACS Omega XXXX, XXX, XXX−XXX

surface morphology (Figure S2); XPS characterization of the catalysts before and after ammonia synthesis (Tables S1 and S2); ammonia production using various catalysts compared with an empty reactor (Figure S3); comparison of the ammonia yield with data from the literature (Table S3); and the temperatures of the catalysts at different positions (Table S4) (PDF)

AUTHOR INFORMATION

Corresponding Author

Rok Zaplotnik − *Department of Surface Engineering, Jozef Stefan Institute, 1000 Ljubljana, Slovenia;* orcid.org/0000-0002-1366-9147; Email: rok.zaplotnik@ijs.si

Authors

Alenka Vesel − *Department of Surface Engineering, Jozef Stefan Institute, 1000 Ljubljana, Slovenia*

Parameswaram Ganji − *Department of Surface Engineering, Jozef Stefan Institute, 1000 Ljubljana, Slovenia*

Gregor Primc − *Department of Surface Engineering, Jozef Stefan Institute, 1000 Ljubljana, Slovenia*

Miha Čekada − *Department of Thin Films and Surfaces, Jozef Stefan Institute, 1000 Ljubljana, Slovenia*

Gregor Dolanc − *Department of Systems and Control, Jozef Stefan Institute, 1000 Ljubljana, Slovenia*

Miran Mozetič − *Department of Surface Engineering, Jozef Stefan Institute, 1000 Ljubljana, Slovenia*

Complete contact information is available at: https://pubs.acs.org/10.1021/acsomega.6c01120

Author Contributions

The manuscript was written through contributions of all authors. All authors have given approval to the final version of the manuscript. All authors contributed equally.

Funding

This research was funded by the Slovenian Research Agency core funding P2-0082 "Thin-film structures and plasma surface engineering". The authors acknowledge partial support from the Republic of Slovenia, Ministry of Higher Education, Science and Innovation, and from the European Union−-NextGenerationEU in the framework of the project HyBReED, which is part of the Slovenian Recovery and Resilience Plan. Views and opinions expressed are, however, those of the authors only and do not necessarily reflect those of the Republic of Slovenia, Ministry of Higher Education, the European Union, or the European Commission. Neither the Republic of Slovenia, the Ministry of Higher Education, Science and Innovation, the European Union, nor the European Commission can be held responsible for them.

Notes

The authors declare no competing financial interest.

ACKNOWLEDGMENTS

Janez Trtnik and Jožko Fišer are gratefully acknowledged for their technical assistance.

REFERENCES

(1) Erfani, N.; Baharudin, L.; Watson, M. Recent advances and intensifications in Haber-Bosch ammonia synthesis process. *Chem. Eng. Process.* **2024**, *204*, No. 109962.

(2) Humphreys, J.; Lan, R.; Tao, S. Development and Recent Progress on Ammonia Synthesis Catalysts for Haber−Bosch Process. *Adv. Energy Sustainability Res.* **2021**, *2*, No. 2000043.

(3) Smith, C.; Hill, A. K.; Torrente-Murciano, L. Current and future role of Haber−Bosch ammonia in a carbon-free energy landscape. *Energy Environ. Sci.* **2020**, *13*, 331−344.

(4) Kyriakou, V.; Garagounis, I.; Vourros, A.; Vasileiou, E.; Stoukides, M. An electrochemical Haber-Bosch process. *Joule* **2020**, *4*, 142−158.

(5) Spatolisano, E.; Pellegrini, L. A. Haber-Bosch process intensification: A first step towards small-scale distributed ammonia production. *Chem. Eng. Res. Des.* **2023**, *195*, 651−661.

(6) Shi, R.; Zhang, X.; Waterhouse, G. I. N.; Zhao, Y.; Zhang, T. The journey toward low temperature, low pressure catalytic nitrogen fixation. *Adv. Energy Mater.* **2020**, *10*, No. 2000659.

(7) Shahed Gharahshiran, V.; Zheng, Y. Sustainable ammonia synthesis: An in-depth review of non-thermal plasma technologies. *J. Energy Chem.* **2024**, *96*, 1−38.

(8) Zhang, J.; Li, X.; Zheng, J.; Du, M.; Wu, X.; Song, J.; Cheng, C.; Li, T.; Yang, W. Non-thermal plasma-assisted ammonia production: A review. *Energy Convers. Manage.* **2023**, *293*, No. 117482.

(9) Zhang, S.; Zhao, Y.; Shi, R.; Waterhouse, G. I. N.; Zhang, T. Photocatalytic ammonia synthesis: Recent progress and future. *EnergyChem* **2019**, *1*, No. 100013.

(10) Ganji, P.; Zaplotnik, R.; Primc, G.; Mozetič, M.; Vesel, A. Roles of Catalysts in Plasma Conversion of N_2 and H_2 to NH_3: Advances, Challenges, and Future Directions. *Energy Fuels* **2025**, *39* (30), 14413−14436.

(11) Ohoyama, H. Vector correlation between the alignment of reactant N_2 ($A\ ^3\sum_u^+$) and the alignment of product NO ($A\ ^2\sum^+$) rotation in the energy transfer reaction of aligned N_2 ($A\ ^3\sum_u^+$) + NO ($X\ ^2\Pi$) → NO ($A\ ^2\sum^+$) + N_2 ($X\ ^1\sum_g^+$). *J. Chem. Phys.* **2013**, *139*, No. 234308.

(12) Han, J.; Park, W.; Kim, J.; Lim, K.-H.; Lee, G.-H.; In, S.; Park, J.; Oh, S.-J.; Nam, S. K.; Sung, D.-Y.; Moon, S. Y. Synthetic molecular spectra modeling for determining rotational, vibrational, and excitation temperatures of low-pressure nitrogen plasma. *Spectrochim. Acta, Part A* **2024**, *304*, No. 123389.

(13) Guerra, V.; Galiaskarov, E.; Loureiro, J. Dissociation mechanisms in nitrogen discharges. *Chem. Phys. Lett.* **2003**, *371*, 576−581.

(14) Volynets, A. V.; Lopaev, D. V.; Rakhimova, T. V.; Chukalovsky, A. A.; Mankelevich, Y. A.; Popov, N. A.; Zotovich, A. I.; Rakhimov, A. T. N_2 dissociation and kinetics of $N(^4S)$ atoms in nitrogen DC glow discharge. *J. Phys. D:Appl. Phys.* **2018**, *51*, No. 364002.

(15) Matveyev, A. A.; Silakov, V. P. Kinetic processes in a highly-ionized non-equilibrium hydrogen plasma. *Plasma Sources Sci. Technol.* **1995**, *4*, 606.

(16) Tatarova, E.; Dias, F. M.; Gordiets, B.; Ferreira, C. M. Molecular dissociation in N_2−H_2 microwave discharges. *Plasma Sources Sci. Technol.* **2005**, *14*, 19.

(17) Mozetič, M. Low-pressure non-equilibrium plasma technologies: scientific background and technological challenges. *Rev. Mod. Plasma Phys.* **2025**, *9* (1), 25.

(18) Zaplotnik, R.; Primc, G.; Paul, D.; Mozetič, M.; Kovač, J.; Vesel, A. Atomic species generation by plasmas. In *Plasma Applications for Material Modification: From Microelectronics to Biological Materials*, 1st ed.; Tabarés, F. L., Ed.; Jenny Stanford Publishing: Singapore, 2021.

(19) Carreon, M. L. Plasma catalytic ammonia synthesis: state of the art and future directions. *J. Phys. D:Appl. Phys.* **2019**, *52*, No. 483001.

(20) Carrasco, E.; Jiménez-Redondo, M.; Tanarro, I.; Herrero, V. J. Neutral and ion chemistry in low pressure DC plasmas of H_2/N_2 mixtures: routes for the efficient production of NH_3 and NH_4^+. *Phys. Chem. Chem. Phys.* **2011**, *13*, 19561−19572.

(21) Hong, J.; Pancheshnyi, S.; Tam, E.; Lowke, J. J.; Prawer, S.; Murphy, A. B. Kinetic modelling of NH_3 production in N_2−H_2 non-equilibrium atmospheric-pressure plasma catalysis. *J. Phys. D:Appl. Phys.* **2017**, *50*, No. 154005.

(22) Primc, G. Generation of neutral chemically reactive species in low-pressure plasma. *Front. Phys.* **2022**, *10*, No. 895264, DOI: 10.3389/fphy.2022.895264.
(23) Booth, J.-P.; Mozetič, M.; Nikiforov, A.; Oehr, C. Foundations of plasma surface functionalization of polymers for industrial and biological applications. *Plasma Sources Sci. Technol.* **2022**, *31* (10), No. 103001.
(24) Draškovič-Bračun, A.; Mozetič, M.; Zaplotnik, R. E- and H-mode transition in a low pressure inductively coupled ammonia plasma. *Plasma Process. Polym.* **2018**, *15* (1), No. 1700105.
(25) Zaplotnik, R.; Drenik, A.; Vesel, A.; Mozetič, M. Ammonia production in a dual crossed atom beam experiment. *Nucl. Fusion* **2023**, *63* (6), No. 066035.
(26) Zaplotnik, R.; Vesel, A.; Mozetic, M. A fiber optic catalytic sensor for neutral atom measurements in oxygen plasma. *Sensors* **2012**, *12* (4), 3857−3867.
(27) Mozetic, M.; Vesel, A.; Drenik, A.; Poberaj, I.; Babic, D. Catalytic probes for measuring H distribution in remote parts of hydrogen plasma reactors. *J. Nucl. Mater.* **2007**, *363*−*365*, 1457−1460.
(28) Notter, D.; Elias Abi-Ramia Silva, T.; Gálvez, M. E.; Bulfin, B.; Steinfeld, A. Thermochemical production of ammonia via a two-step metal nitride cycle − materials screening and the strontium-based system. *Mater. Horiz.* **2024**, *11*, 4054−4063.
(29) Vojvodic, A.; Medford, A. J.; Studt, F.; Abild-Pedersen, F.; Khan, T. S.; Bligaard, T.; Nørskov, J. K. Exploring the limits: A low-pressure, low-temperature Haber−Bosch process. *Chem. Phys. Lett.* **2014**, *598*, 108−112.
(30) Medford, A. J.; Vojvodic, A.; Hummelshøj, J. S.; Voss, J.; Abild-Pedersen, F.; Studt, F.; Bligaard, T.; Nilsson, A.; Nørskov, J. K. From the Sabatier principle to a predictive theory of transition-metal heterogeneous catalysis. *J. Catal.* **2015**, *328*, 36−42.
(31) Iwamoto, M.; Akiyama, M.; Aihara, K.; Deguchi, T. Ammonia synthesis on wool-like Au, Pt, Pd, Ag, or Cu electrode catalysts in nonthermal atmospheric-pressure plasma of N_2 and H_2. *ACS Catal.* **2017**, *7* (10), 6924−6929.
(32) Kitchamsetti, N.; de Barros, A. L. F.; Mhin, S. Transition metal nitrides: Multifunctional catalysts and energy materials with tailorable architectures. *Small Sci.* **2025**, *5* (11), No. 2500331.
(33) Awaji, M.; Pentecoste-Cuynet, L.; Noël, C.; Gries, T.; Belmahi, M.; Belmonte, T. Ammonia cracking by microwave plasma under reduced pressure. *Int. J. Hydrogen Energy* **2025**, *119*, 377−385.
(34) John, J.; Lee, D.-K.; Sim, U. Photocatalytic and electrocatalytic approaches towards atmospheric nitrogen reduction to ammonia under ambient conditions. *Nano Convergence* **2019**, *6*, No. 15.
(35) Skúlason, E.; Bligaard, T.; Gudmundsdóttir, S.; Studt, F.; Rossmeisl, J.; Abild-Pedersen, F.; Vegge, T.; Jónsson, H.; Nørskov, J. K. A theoretical evaluation of possible transition metal electro-catalysts for N_2 reduction. *Phys. Chem. Chem. Phys.* **2012**, *14*, 1235−1245.

https://doi.org/10.1021/acsomega.6c01120
ACS Omega XXXX, XXX, XXX−XXX